

## Applications of Unmodified Geothermal Silica for Protein Extraction

Halldor G. Svavarsson<sup>1,2,\*</sup>, Hronn Arnardottir, Sigurbjorn Einarsson<sup>1</sup>, Albert Albertsson<sup>3</sup>, Asa Brynjolfsdottir<sup>1</sup>

<sup>1</sup> Blue Lagoon Ltd. Iceland, <sup>2</sup>School of science and engineering, Reykjavík University, Iceland, <sup>3</sup>HS Energy, Grindavik, Iceland

\* [halldorsv@ru.is](mailto:halldorsv@ru.is)

**Keywords:** Geothermal silica, chromatographic, adsorption, protein separation.

### ABSTRACT

Silica deposits are being considered an undesirable byproduct of geothermal power production and large quantities of it can be extracted from geothermal fluid. Here we introduce an adsorption application of silica, precipitated out of geothermal fluid discharged from a geothermal powerplant in Svartsengi on the Reykjanes peninsula in Iceland. Its ability to separate protein from biomass was manifested by selective adsorption of blue colored protein, *C-phycocyanin*, from disrupted coccoid blue-green algae cultivated in geothermal fluid at the Blue Lagoon Research Center. Upon adsorption and subsequent elution the purity of the extracted protein, measured as the ratio of the light absorbance of 620 and 280 nm, increased considerably or up to five times the original value. Analysis of the silica, using scanning electron microscopy, X-ray diffractometry and Brunauer–Emmett–Teller (BET) adsorption confirmed it is highly porous, has a high specific surface area and is amorphous. Its adsorption ability is attributed to this high surface area and open structure. Our results could facilitate utilization of a mostly unused byproduct of geothermal powerplants as chromatographic material.

### 1. INTRODUCTION

#### 1.1 Geothermal Silica

The geothermal powerplant HS-Energy is located in Svartsengi on the Reykjanes peninsula, south-west Iceland on a sequence of lava flows (see Fig. 1), the youngest being roughly 800 years old (Saemundsson et al., 2010).



**Figure 1. Left:** photograph of the Blue Lagoon and HS Energy powerplant. **Right:** photograph of the HS Energy powerplant from different angle and at higher magnification.

The geological structure is further characterised by interlayers of scoria and hyaloclastite reflecting interglacial and glacial periods. Since the interlayers are highly porous and permeable, they allow seawater to percolate deep into their aquifers where it heats up and mixes with meteoric water (Arnórsson, 1995). Geothermal wells drilled through the lava flows to depths of up to 2,000 m discharge a mixture (here referred to as geothermal fluid) of 2/3 seawater and 1/3 meteoric water with a temperature of about 240°C. Due to the high temperature, the geothermal fluid contains a high concentration of silicon (Si) when it enters the wells. Originally, the silicon is present in the hot geothermal fluid as silicic acid ( $\text{SiO}_3(\text{OH})_{4-2x}$ )<sub>n</sub> but upon cooling it precipitates as a three-dimensional network of coagulated primary silica ( $\text{SiO}_2$ ) particles. The primary particles grow up to few nanometers in size before they coagulate to form aggregated clusters with high specific surface area. This high surface area makes the  $\text{SiO}_2$  a suitable candidate for adsorption and catalytic applications. Steam from the flashed geothermal fluid is used to produce electricity (output power of ~75 MW<sub>e</sub>). The residual liquid is used in a heat exchange process (output power of ~150 MW<sub>i</sub>) to heat up freshwater for district heating of local communities of roughly 20,000 habitants. This heat exchange process limits the minimum temperature for heat extraction of the geothermal fluid to about 90°C. Most of the spent geothermal fluid is reinjected into the geothermal reservoir (~ $6 \times 10^6 \text{ m}^3$  annually) but some of it (~ $1.2 \times 10^6 \text{ m}^3$  annually) is discharged on the adjacent surface where it forms the Blue Lagoon (Grether-Beck et al., 2008; Petursdottir et al., 2009). A small fraction of the discharged fluid is bypassed to  $4 \times 40 \text{ m}^3$  sedimentation tanks (shown in Fig. 2) at the Blue Lagoon where it cools to ambient temperature.



**Figure 2. Silica sedimentation tanks at the Blue Lagoon**

Upon cooling the fluid becomes supersaturated in respect to the silicic acid which in turn precipitates as amorphous  $\text{SiO}_2$ . The pH of the resulting supernatant is  $7.7 \pm 0.2$ , slightly higher than the pH of the Blue Lagoon which is  $7.5 \pm 0.2$ . At  $90^\circ\text{C}$ , the geothermal fluid contains about 600 ppm  $\text{SiO}_2$  and thus the  $7 \times 10^6 \text{ m}^3$  of liquid being discharged and reinjected annually carries about 4,000 tonnes. At  $10\text{--}15^\circ\text{C}$ , a realistic ambient temperature, the  $\text{SiO}_2$  concentration has dropped by roughly an order of magnitude (Fleming and Crerar, 1982) and thus a precipitation of over 3,000 tons could potentially be harnessed annually from fluid discharged from the HS Energy facility alone.

Few authors have reported on practical applications of modified geothermal  $\text{SiO}_2$  and still fewer on applications of unmodified  $\text{SiO}_2$ . A possible use of geothermal  $\text{SiO}_2$  as a filler in paper (Johnston et al., 2004) and as a precursor for silicates (Gallup et al., 2003) has been described. In both cases the precipitation conditions had to be controlled.

### 1.2 Chromatographic Silica

Silica gel ( $\text{SiO}_2 \cdot x\text{H}_2\text{O}$ ) is widely used as an adsorbent in chromatographic columns for isolation and purification of compounds from a mixture. One of the most common methods for the analysis of basic pharmaceuticals is liquid chromatography (McKeown et al., 2001), which conventionally relies on synthetic silica and silica derivatives as the stationary phase. The production of synthetic chromatographic silica typically involves several chemical reaction steps followed by a series of after-treatment processes (Hoffmann et al., 2006; Zhang et al., 2009). In this paper we report chromatographic application of unmodified geothermal silica. A comparison to sintered geothermal silica is given.

### 1.3 Phycocyanin

The Blue Lagoon is a specific geothermal biotope known for its unique microbial ecosystem (Petursdottir and Kristjansson, 1997; Petursdottir et al., 2009). It was created in 1976 during operation of the nearby geothermal power plant now called HS Energy. The lagoon is one of most prestigious geothermal spas in the world, having roughly 600 thousand visitors annually. It contains about  $6,000 \text{ m}^3$  of geothermal fluid that is gradually replenished every 40 h while the temperature remains constant at  $38 \pm 1^\circ\text{C}$ . A photograph of the Blue Lagoon spa is shown in Fig. 3.



**Figure 3. A photograph of the Blue Lagoon geothermal spa. Steam rising up of HS Energy powerplant is seen in the background.**

The coccoid blue-green algae, *Cyanobacterium aponinum*, one of the dominating species in the microbial ecosystem of the Blue Lagoon, is used in this research. A blue-colored protein, Phycocyanin (C-PC), is a water-soluble photosynthetic pigment found in blue-green algae. It is an accessory pigment to the green-colored pigment chlorophyll, also found in blue-green algae. Together they are an essential component of the algae's light harvesting system. Among many interesting applications of C-PC is its use as a fluorescent marker of cells and macromolecules and as a natural colorant in food and cosmetic products, replacing synthetic dyes, which are often unsafe or even toxic. C-PC has also been shown to exhibit bio-activity (Eriksen, 2008) which makes it an excellent

choice as an additive in food and pharmaceutical products. However, the use of C-PC in these products is dependent on obtaining the appropriate grade of purity. The purity of C-PC can be roughly estimated as the ratio between the light absorbance at  $\lambda = 620$  nm and 280 nm ( $A_{620}/A_{280}$ ), where  $A_{620\text{nm}}$  is the maximum absorbance of C-PC and  $A_{280\text{nm}}$  is the total absorbance of proteins. A purity of 0.7 is considered food grade, 3.9 reactive grade and greater than 4.0 analytical grade (Rito-Palomares et al., 2001). Despite the many possible applications of C-PC, its use is limited by the high cost of extraction and purification. Most of the purification methods involve a sequence of operations that include precipitation, centrifugation, dialysis, ion-exchange and gel filtration chromatography and chromatography on hydroxyapatite (Rito-Palomares et al., 2001). The purification cost has been estimated at 50-90% of the total production cost (Patil et al., 2006). Improvements in the purification procedure can therefore lead to a significant reduction in the production cost. C-PC is unstable to heat and light in an aqueous solution and denatures at temperatures above 45°C which puts constraints on the possible processing methods that can be used. In the experiments described in this paper, unmodified geothermal  $\text{SiO}_2$  precipitated from Blue Lagoon geothermal fluid was used as an alternative to other chromatographic materials to extract C-PC from the coccoid blue-green alga, *cyanobacterium aponinum*. When  $\text{SiO}_2$  agglomerates were immersed in a saline solution of a ruptured cell mass, the C-PC was selectively adsorbed on it. The retained C-PC was released from the  $\text{SiO}_2$  adsorbent by desalination with deionized water.

## 2. EXPERIMENTAL PROCEDURE

### 2.1. Algae Cultivation

Blue-green algae, isolated from the Blue Lagoon, were cultivated in a semi-continuous mode in a 1.2 m<sup>3</sup> tubular photobioreactor at 45°C at the Blue Lagoon Research and Development Center in Iceland. A photograph of the cultivation system and an optical micrograph of the algae are shown in Fig. 4 a) and 4 b) respectively.

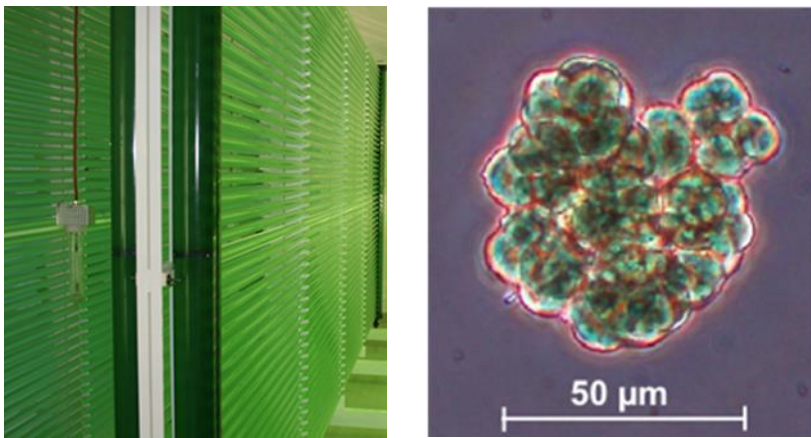


**Figure 4. Left: photograph of the tubular photobioreactor used in the experiment. Right: micrograph of the blue-green algae cultivated in the photobioreactor**

The cultivation media was geothermal fluid with 0.3% mass/vol Cell-hi WP nutrient. Illumination was provided by high pressure sodium light (160  $\mu\text{E}/\text{m}^2/\text{s}$ ). A fixed pH of 7.5 was maintained by regulating the  $\text{CO}_2$  gas feed rate during growth. Just after harvesting, the algae concentration of the culture suspension was increased to 12.2% wt. dry weight by passing it through a Westfalia centrifugal separator. The enriched suspension was homogenized using a 900 W ultrasonic cell crusher at 20 kHz (SYJ900-D from Sharpertek) with a duty cycle of 2 s on and 3 s off (a total of 30 min/liter of suspension). Subsequently, the solution was centrifuged at 3200 g. The supernatant, referred to as crude extract, was collected.

### 2.2. Chromatographic Silica

Raw materials used for the chromatographic recovery of C-PC consisted of geothermal  $\text{SiO}_2$  (referred to as BL-silica) and geothermal salt (referred to as BL-salt). The chemical composition of the BL-silica and the BL-salt was determined by inductively coupled plasma mass spectrometry (ICP-MS). The precipitated BL-silica was removed from the sedimentation tank and fed into a filtration press at a pressure of 2 bar. The resulting filter cake was dried at 60°C, crushed manually and sieved. After removal of the BL-silica, the BL-salt was prepared by drying the supernatant. The characteristics of the BL-silica (ground in a mortar), before and after sintering at 1000°C for 2 h, was determined using a scanning electron microscope (SEM) and by measuring the specific surface area (BET), t-plot area and Barrett-Joyner-Halenda (BJH) average adsorption pore width (Micromeritics TriStar 3000 Surface Area and Porosity Analyzer). The mineralogy of the BL-silica was determined by X-ray diffraction analysis (XRD: Bruker AXS).

### 2.3. Protein Extraction

It was observed that the BL-silica could only bind C-PC in a saline solution and not in deionized water. Subchapter 2.3.1 describes the effect of salt concentration on binding capacity of the BL-silica. The concentration of C-PC was determined using Eq. (1) (Mishra et al., 2008),

$$C_{\text{C-PC}} = (A_{620} - 0.474A_{652})/(5.34) \text{ [mg/ml]} \quad (1)$$

where  $A_{620}$  and  $A_{652}$  are the light absorption values at 620 and 652 nm, respectively.

Subchapters 2.3.2 and 2.3.3 describe two different alternatives for the protein extraction: the first one (Method 1) is a continuous process where the crude extract is fed through a column filled with coarse silica agglomerates and the second one (Method 2) is a batchwise process where the crude extract is mixed with fine silica agglomerates and centrifuged.

### 2.3.1 Effect of salt concentration on the binding capacity

A following sample series was prepared: BL-silica was washed with deionized water in a Buhner funnel after which it was dispersed with an ultrasonic probe. The resulting silica suspension had 21.6 % dry content. 1.0 ml of the silica suspension and 1.0 ml of a C-PC solution (750 mg C-PC/ml) were put together in 10 ml volumetric flasks that were filled up with BL-salt solution of different concentrations and centrifuged. The C-PC's concentration in the supernatant was measured in accordance to equation (1). A comparison between the observed amount of C-PC in the supernatant and the amount known to be in centrifuged volume was used to calculate the binding ratio.

### 2.3.2. Method 1

BL-silica agglomerates, ranging in size from 0.2 to 0.7 mm, were packed in a 30 cm tall plexiglas column with a diameter of 5 cm. The column was flushed with 500 ml of BL-salt solution (25% wt. salt) and subsequently loaded with 190 ml crude extract (see *Algae cultivation* above) at a pressure of 0.4 bar. Afterwards the green colored chlorophyll was washed off by running 2.2 l of BL-salt solution (25% wt. salt) through the column. Subsequently the C-PC was eluted by running deionized water through it. The pressure was gradually increased from 0.4 to 0.6 bar during running of the BL-salt solution and the eluent. The experiment was repeated using sintered BL-silica (1000°C/2h) as the stationary adsorbent instead of unsintered BL-silica.

### 2.3.3. Method 2

BL-silica agglomerates smaller than 125  $\mu$ m in diameter were mixed with the crude extract and a BL-salt (25% wt.) solution. The C-PC discharge was accomplished batchwise by alternating cycles of centrifugation and addition of deionized water. A 100 ml crude extract (see *Algae cultivation* above) was mixed with 10 ml of saturated BL-salt solution (approximately 0.36 g salt per ml) and 20 g of BL-silica and then centrifuged. The supernatant was discarded and the sediment was slurried in 50 ml of saline solution (40 ml of deionized water and 10 ml of saturated BL-salt solution) and centrifuged again. This step of slurring the sediment and centrifuging was repeated with deionized water in discrete volumes of 10 ml. The supernatant, containing eluted C-PC, was collected after each step. Absorption values and absorbance spectra of the supernatant (eluent) and the crude extract were measured using a UV-visible Camspec M350 spectrophotometer.

## 3. RESULTS AND DISCUSSION

### 3.1 Protein extraction

#### 3.1.1 Effect of Salt Concentration on the Binding Capacity of Silica

The relative binding of C-PC versus BL salt concentration is visualized in Fig 5. A roughly linear relation is observed for up to about 25% salt concentration after which the curve flattens out.

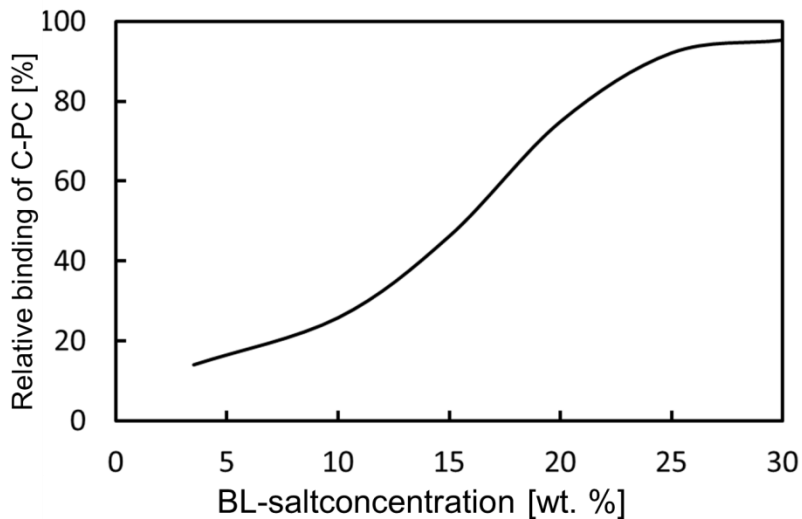


**Figure 5. Binding of C-PC to BL-silica versus concentration of BL-salt in the solution.**

At the salt concentration of 25%, the binding capacity measures as 92%. It can thus be concluded that a minimum concentration of 25% wt. is needed to obtain saturation in the silica's binding capacity.

#### 3.1.2 Method 1

The concentration of C-PC versus elution volume is displayed with the black solid line in Fig. 6.

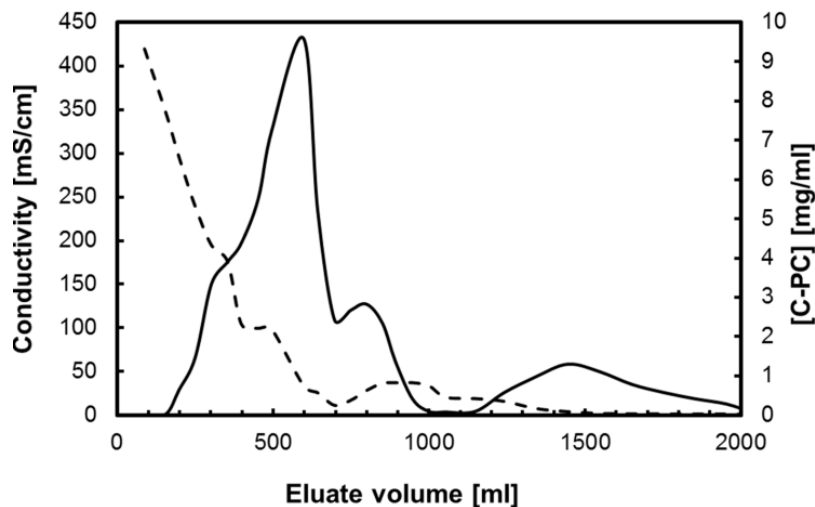


**Figure 6. Electrical conductivity (dotted line) and C-PC's concentration (solid line) versus volume of deionized water passing the BL-silica column.**

As seen, a certain minimum volume of the deionized water ( $\sim 150$  ml) is needed before the C-PC's discharge starts. After this threshold level is reached, the C-PC's concentration rises roughly linearly with volume until it peaks at 600 ml after which it gradually reduces. Some noticeable features are a dip in the curve at 700 ml and blunt minima around 1100 ml. Both these features may be attributed to breakdown and decomposition of the silica agglomerates while passing the eluent through the column at elevated pressure. Consequently C-PC molecules being trapped in the agglomerate's pores would be more easily discharged. The salt removal rate of the silica columns was measured indirectly by monitoring the conductivity of the eluate (dotted line in Fig. 6) with Hanna Hi 9033 portable conductivity meter. As the main source of ions in the eluate arrives from the BL-salt, the conductivity is assumed to be proportional to the salt concentration. As to expect the conductivity gradually decreases with increasing eluate volume and it reaches a minimum at 700 ml, shortly after the C-PC concentration has peaked. A small increment observed at the interval of 700-1000 ml is directly related to the increased discharge rate of C-PC over the same interval.

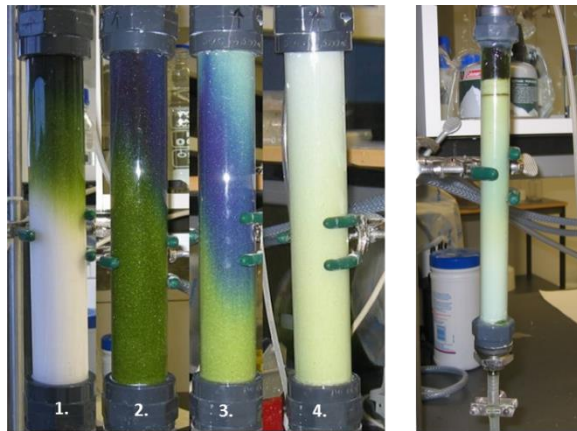


**Figure 7. Left:** Separation of C-PC in a column at different stages in chronological order: (1) at early stage of the loading, (2) after loading with 190 ml crude extract, (3) after flushing with 2.2 l of brine solution (25% BL-salt in deionized water), and (4) after elution with 2.0 l deionized water. **Right:** column with sintered BL-silica after loading and subsequent flushing with brine solution. Apparently no C-PC was retained.

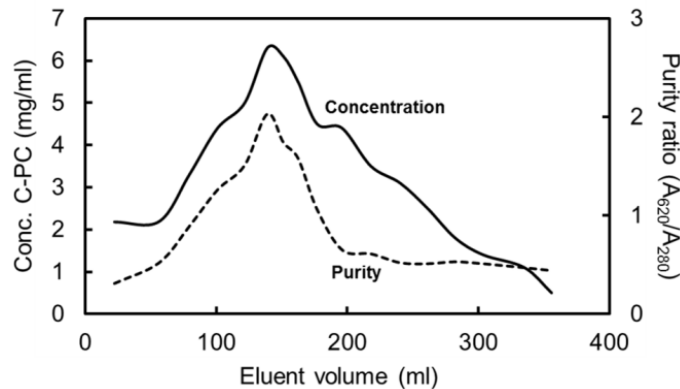
It is evident from these results that the collected eluate volume will contain considerable amount of salt which is undesirable in respect to the concentration of the final product (pure and concentrated C-PC). An extra processing step, such as dialysis, would therefore be needed if the presence of salt is undesirable in the end product. The proceeding of the column's loading and elution is visualized in chronological order in Fig. 7 (left). As seen, the green colored chlorophyll flows through the column while the C-PC is retained at the stationary BL-silica. A good separation of C-PC was obtained, with a net 3-fold increment in purity. The column, however, degraded due to compression of the agglomerates during running of the eluent making the BL-silica adsorbent disposable. An attempt to strengthen the  $\text{SiO}_2$  agglomerates with sintering resulted in a total loss of performance (see Fig. 7 (right)) accompanied by a decrease of its specific surface area from 60 to  $1 \text{ m}^2$  (see Table 1).

**Table 1.** Surface characteristics of BL-silica.

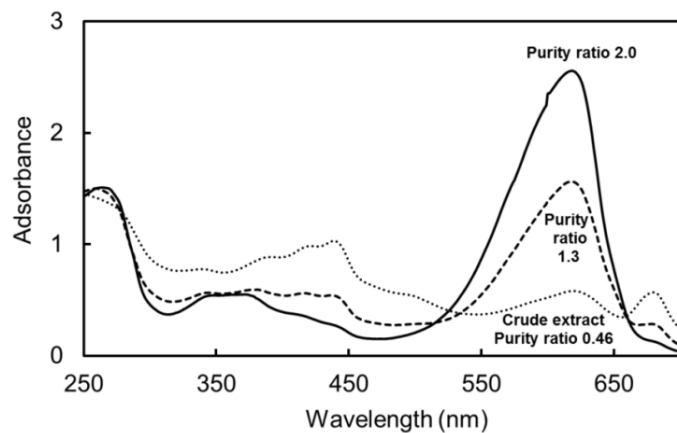
BL-silica	BET spec. surf. area [m <sup>2</sup> /g]	Micropore surf. area t-Plot [m <sup>2</sup> /g]	Vol. of pores with diameter 1.7 – 300 nm [cm <sup>3</sup> /g]	BJH adsorption av. pore width [nm]
Unsintered	50	6	0.24	23
Sintered	1	0.3	0.001	N/A

**3.2.2 Method 2**

A graphical interpretation of the results is given in Fig. 8 where the C-PC's concentration and PR are shown as a function of the eluent volume.

**Figure 8.** Concentration of C-PC (dashed line) and C-PC purity (solid line) as a function of eluent volume.

Both lines rise roughly linearly with increasing eluent volume up to ~140 ml. At higher volumes the concentration decreases throughout the elution while the purity line flattens out rather abruptly at volumes above ~200 ml. The maxima of the PR, ~2.0, and the  $C_{C-PC}$ , 6.3 mg/ml, appear at the same eluent volume. Corresponding values for the crude extract are 0.46 and 18.2 mg/ml, respectively. As always, there is a trade-off between the purity of the protein and its recovery rate. Accumulated volumes with PR = 2.0, 1.3 and 1.0 were collected with 4%, 31% and 50% recovery respectively. Absorption spectra, in the range of 250-700 nm, of collections with different purities are shown in Fig. 9. A spectrum of the crude extract is shown for comparison.

**Figure 9.** Absorption spectra for algae extracts of different purity: crude extract (dotted line), PR = 1.3 (dashed line), and PR = 2.0 (solid line).**3.2 Morphology Analyses of the Chromatographic Silica**

Values of the specific surface area, micropore surface area, pore volume and average adsorption pore width of the BL-silica, before and after sintering are given in Table 1. Table 2 shows the chemical composition of the BL-silica and the BL-salt.

**Table 2.** Chemical composition of BL-silica and BL-salt (wt. %).

Component	SiO <sub>2</sub>	Cl	Na	Ca	K	Mg	Total
BL-silica	92.9	3.9	2.2	0.49	0.39	< 0.1	99.9
BL-salt	0.02	58.7	34.0	1.83	1.75	< 0.1	96.3

The XRD patterns of BL-silica prior to sintering and after sintering are shown in Fig. 10. The amorphous structure, prior to sintering, is clearly demonstrated by the absence of sharp diffraction peaks. The dry SiO<sub>2</sub> powder contains ~7 wt. % of salt (mainly NaCl). Sharp peaks in Fig. 10 at  $2\theta = 31.75^\circ$  and  $45.48^\circ$  are due to crystalline NaCl present in the BL-silica. After sintering, a strong and sharp peak has appeared at  $2\theta = 22^\circ$ , indicating some of the amorphous SiO<sub>2</sub> has been converted to a crystalline form of SiO<sub>2</sub> (cristobalite).

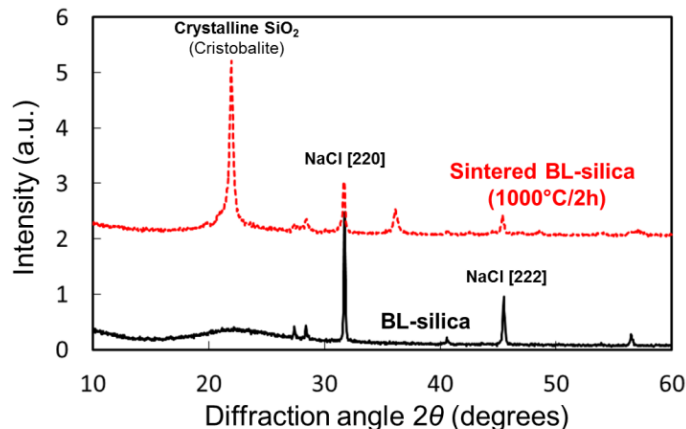


**Figure 10.** X-ray diffraction pattern of BL-silica before (black solid line) and after sintering at 1000°C for 2 hours (red dotted line).

Fig. 11 displays SEM images of BL-silica agglomerates before and after sintering. Prior to sintering a porous surface composed of primary particles with diameters ranging from 20 nm to 90 nm is seen. According to Icopini et al. (2005), who investigated oligomerization of SiO<sub>2</sub> as a function of its concentration, ionic strength and pH in natural brine solutions, coagulation occurs when the SiO<sub>2</sub> particles reach ~3 nm in size. Our values of 20-90 nm are much larger than the value they give. However, it must be taken into account that in their case the silica precipitation was triggered by change in the pH whereas in our case it was triggered by a change in temperature. Upon sintering the particles have grown and apparently fused together. The porous appearance is no longer visible; instead a glass-like surface has formed. These structural changes may, in part, be attributed to the salt present in the BL-silica. As the sintering temperature of 1000°C is above the melting point of NaCl (801°C), the SiO<sub>2</sub> could have been covered with the molten salt which solidifies upon cooling. Additional phases, formed by reactions of the SiO<sub>2</sub> and the molten salt, may also be present. A further indication of the morphological changes occurring in the sintered SiO<sub>2</sub> is the observed decrease in the pore volume, from 0.24 to 0.001 cm<sup>3</sup>/g (Table 1). This is consistent with the observed loss of performance of the SiO<sub>2</sub> after sintering. The average pore width of 23 nm is several times the size of the C-PC protein molecule (Fisher et al., 1980). These facts could explain the selective adsorption of C-PC from the crude extract containing chlorophyll and C-PC.

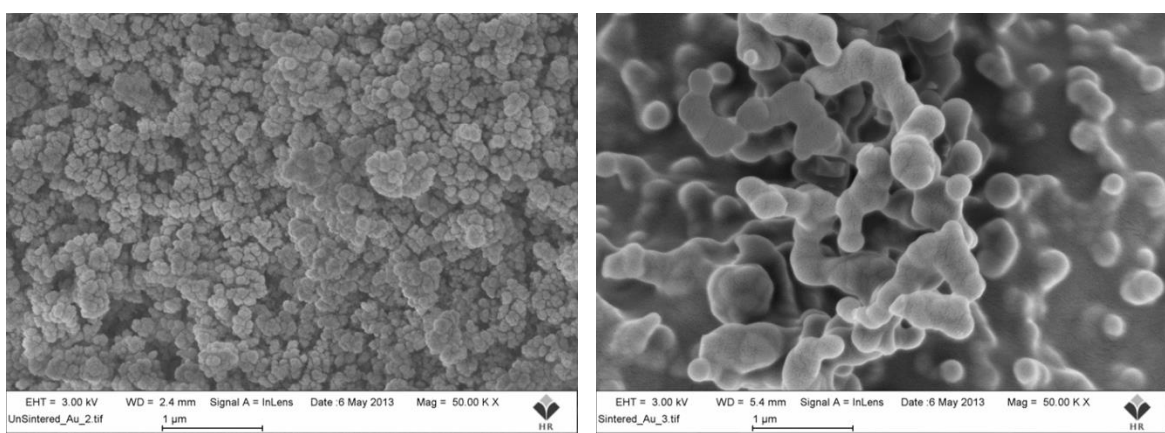


**Figure 11.** SEM images of the BL-silica. Left: before sintering, Right: after sintering.

#### 4. CONCLUSIONS

A use of geothermal  $\text{SiO}_2$  as a chromatographic material was described. Its ability to adsorb protein molecules was demonstrated by the separation of C-PC from disrupted blue-green algae mass. A critical factor controlling the adsorption capability is the high specific surface area of the silica as confirmed by loss of performance upon sintering. A geothermal-salt concentration in excess of 25% wt. was needed to assure efficient adsorption. The process described here is viable as a simple, ecological and inexpensive first step in the purification and separation of natural proteins by utilizing geothermal resources.

#### REFERENCES

Arnórsson S.: Geothermal systems in Iceland: Structure and conceptual models .1. High-temperature areas, *Geothermics* **24**, (1995), 561-602.

Eriksen N.T.: Production of phycocyanin - a pigment with applications in biology, *Appl. Microbiol. Biot.* **80**, (2008), 1-14.

Fisher R.G., Woods N.E., Fuchs H.E., and Sweet R.M.: Three-dimensional structures of C-Phycocyanin and B-Phycoerythrin at 5-A resolution, *J. Biol. Chem.* **255**, (1980), 5082-5089.

Fleming B., Crerar D.: Silicic acid ionization and calculation of silica solubility at elevated temperature and pH application to geothermal fluid processing and reinjection, *Geothermics* **11**, (1982) 15-29.

Gallup D.L., Sugiaman F., Capuno V., and Manceau A.: Laboratory investigation of silica removal from geothermal brines to control silica scaling and produce usable silicates, *Appl. Geochem.*, **18**, (2003) 1597-1612.

Grether-Beck S., Muhlberg K., Brenden H., Felsner I., Brynjolfsdottir A., Einarsson S., Krutmann J.: Bioactive molecules from the Blue Lagoon: in vitro and in vivo assessment of silica mud and microalgae extracts for their effects on skin barrier function and prevention of skin ageing, *Exp. Dermatol.*, **17**, (2008), 771-779.

Hoffmann F., Cornelius M., Morell J., and Froeba M.: Silica-based mesoporous organic-inorganic hybrid materials, *Angew. Chem. Int. Edition* **45**, (2006), 3216-3251.

Icopini G.A., Brantley S.L., and Heaney P.J.: Kinetics of silica oligomerization and nanocolloid formation as a function of pH and ionic strength at 25 degrees C, *Geochim. Cosmochim. AC.*, **69**, (2005) 293-303.

Johnston J.H., McFarlane A.J., Borrman T., and Moraes J.: Nano-structured silica and silicates – new materials and their applications in paper, *Curr. Appl. Phys.*, **4**, (2004) 411-414.

McKeown A., Euerby M., Lomax H., Johnson C., Richie H., and Woodruff M.: The use of silica for liquid chromatographic/mass spectrometric, *J. Sep. Sci.*, **24**, (2001) 835-842.

Mishra S.K., Shrivastav A., and Mishra S.: Effect of preservatives for food grade C-PC from spirulina platensis, *Process Biochem.*, **43**, (2008) 339-345.

Patil G., Chethana S., Sridevi A., and Raghavarao K.: Method to obtain C-Phycocyanin of high purity, *J. Chromatogr. A*, **1127**, (2006) 76-81.

Petursdottir S.K., Bjornsdottir S.H., Hreggvidsson G.O., Hjorleifsdottir S., and Kristjansson J.K.: Analysis of the unique geothermal microbial ecosystem of the Blue Lagoon, *FEMS Microbiol. Ecol.*, **70**, (2009) 425-432.

Petursdottir S.K., and Kristjansson J.K.: *Silicibacter lacuscaerulensis* gen. nov., sp. nov., a mesophilic moderately halophilic bacterium characteristic of the Blue Lagoon geothermal lake in Iceland, *Extremophiles*, **1**, (1997) 94-99.

Rito-Palomares M., Nunez L., and Amador D.: Practical application of aqueous two-phase systems for the development of a prototype process for C-Phycocyanin recovery from spirulina maxima, *J. Chem. Technol. Biot.* **76**, (2001) 1273-1280.

Saemundsson K., Johannesson H., Hjartarson A., Kristinsson S.G., and Sigurgeirsson M.A.: Geological map of southwest Iceland (1:100 000), Iceland GeoSurvey, Iceland (2010).

Zhang A., Xiao C., Xue W., and Chai Z.: Chromatographic separation of cesium by a macroporous silica-based supramolecular recognition agent impregnated material, *Sep. Purif. Technol.*, **66**, (2009) 541-548.